DOI 10.14622/Advances_49_2023_08

Numerical investigation of the lateral movement of doctor blades in gravure printing

Christian Sauder, Tobias Steger, Alina Sersch and Peter Gust

University of Wuppertal, School of Mechanical Engineering and Safety Engineering, Chair of Engineering Design,
Gaußstr. 20, 42119 Wuppertal
E-mails:csauder@uni-wuppertal.de;tobias.steger@uni-wuppertal.de;alina.sersch@uni-wuppertal.de;peter.gust@uni-wuppertal.de

Short abstract

An alternating lateral movement is usually applied to doctor blades to even out wear in gravure printing. This movement leads to an increased load on the doctor blade and can result in damage to the blade edge and thus lead to misprints. The phenomenon is well known to the printing community, but most analytical and numerical models of the doctoring process reduce it to a 2D cross section and are not, therefore, effective in investigating the problem. This study investigates the changes in load during the movement of the doctor blade and the feasibility of using simple shell elements for the given task. One finding is that this simulation approach contributes to the understanding of the doctor blade's lateral movement, especially its displacement. The limitations of the approach are recognised, and future options for improving stress analysis and other physical effects are given.

Keywords: finite element analysis, shell element, doctoring, printing proofer, tip cracking

1. Introduction and background

According to Kipphan (2001) the patterns to be transferred to the substrate in gravure printing are engraved into the surface of a chromed gravure cylinder. The engraved cells are flooded with ink by immersing and rotating the cylinder in a reservoir. The excess ink is then wiped off the unengraved areas by a doctor blade before the substrate is wetted by pushing it into the engraved cells with the help of an impression roller.

The printing quality of the gravure printing process is affected by a large number of parameters (Bohan, Claypole and Gethin, 2000). One important component of a gravure printing press is the doctoring unit with the doctor blade and a backup blade fixed in a blade holder (Swedev AB, Munkfors/S, 2011). The doctoring unit is pneumatically actuated and the doctor blade is pressed against the gravure cylinder. As the doctor blade slides over the chromed surface of the gravure cylinder, it inevitably wears out (Hanumanthu, 1999); in the worst case, high loads can damage the blade's tip (Swedev AB, Munkfors/S, 2011). To even out wear on the doctor blade, the doctoring unit is moved alternately in transverse directions (Ollech, 1993). The literature reports the use of different numerical and analytical models in order to understand the relations of process parameters on the doctoring step in gravure printing. A recent overview is given by Bitsch (2020). Most of these models are reduced to represent a 2D cross section of the doctoring unit, so the effects in the transverse direction are not investigated thoroughly. Scheuter and Bognar (1968) presented an analytical model of a doctor blade utilizing the Kirchhoff-Love theory of thin plates. They investigated the loading and deflection of the blade with respect to shape deviations of the gravure cylinder. Hoang and Ko (2015) conducted a numerical examination of the downward deflection of a doctor blade into an engraved parallel groove. They varied the width of the groove and the doctoring pressure and investigated the effects on cell filling and print quality.

To further understand the doctor blade's behaviour in the transverse direction, we have introduced a new simplified model that also covers the alternating movement of the doctoring unit. This study investigates the global loads and deflections on the doctor blade and support blade, with special interest in the loads at the ends of the gravure cylinder. In addition, it investigates the feasibility of simple shell elements for the given task and the need for sub-modelling techniques for local effects.

2. Materials and methods

2.1 Materials

A gravure printing proofer (Moser HS 157) was chosen as the subject of this research, since it comprises all components of interest and is equipped with an eccentric drive for the lateral movement of the doctoring unit. The device is shown in Figure 1a; its general specifications are given in Table 1. Figure 1b provides a CAD model of the sub-assembly of the doctoring unit and gravure cylinder.

a)

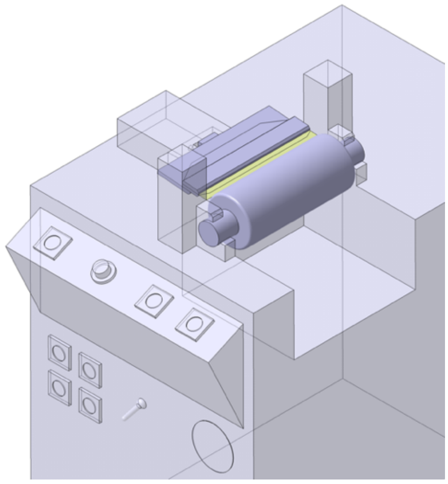

b)

Figure 1: (a) Gravure printing proofer (Moser HS 157), (b) CAD model of the printing proofer with doctoring unit and gravure cylinder

Table 1: Specifications of the gravure printing proofer (Moser HS 157)

Specification	**Value**	**Unit**
Printing speed	10–60	m·min^{-1}
Total stroke of doctoring unit	10	mm
Max. doctoring pressure (D50/d22 piston)	2.5	bar
Printing format	297 × 210	mm
Width of doctoring unit	275	mm
Width of gravure cylinder	260	mm

The doctoring unit consists of a rocker, a support plate, and an upper and lower clamping plate, as well as the doctor blade and support blade. Both blades have been modelled as mid-surfaces of the actual blade bodies, neglecting the cut at the tip of the doctor blade. Figure 2 shows the dimensions of the doctoring setup. The doctor blade and support blade protrude 20 mm and 10 mm respectively from the clamping plates and meet the gravure cylinder at a tangent angle of 65°. Their material thicknesses are 0.2 mm and 0.5 mm respectively. The edge of the gravure cylinder is rounded off with a 5 mm radius, and a 1° slope extends 10 mm from the sides. To relieve the doctor blade at the ends of the gravure cylinder, the edges of the support blade are bevelled to effectively extend the gravure cylinder's ends by 10 mm inwards.

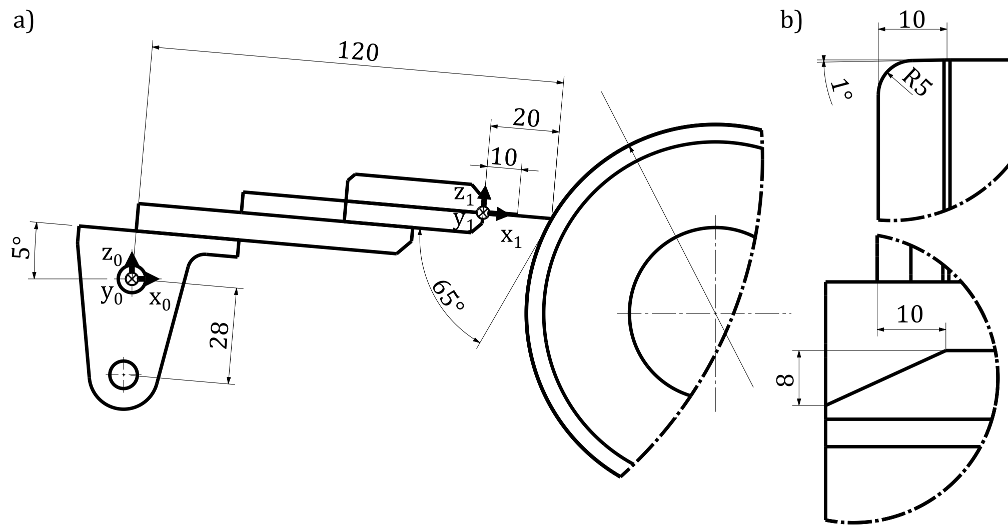

Figure 2: Sketch of the doctoring unit: (a) cross section of the doctor blade unit and the gravure cylinder, (b) detailed view of the end of the gravure cylinder and the edge of the support blade

2.2 Finite element analysis of the doctor blade and support blade

The numerical investigation of the doctoring process is carried out by a static finite element analysis of the doctor blade unit using ANSYS Mechanical 2020 R2.

2.2.1 Material properties and meshing

The doctor blade and support blade are modelled as flexible bodies, while all other bodies are defined as rigid. Steel was assigned as the material of the flexible bodies with a Young's modulus $E = 210 \times 10^3$ MPa and a Poisson's ratio $\nu = 0.3$. Four-node elements are used for meshing both bodies with six degrees of freedom at each node (SHELL 181). This allows the evaluation of membrane and bending stresses. A structured trapezoid-based mesh is used to receive rectangular shaped elements for all sections of the doctor blade and most sections of the support blade. Only in the area of the bevelled edges of the support blade are other trapezoid shapes accepted. The mesh size has been chosen accordingly to give a reasonable resolution and the aspect ratio has been checked to avoid geometric locking effects. Element sizes chosen were 0.2 mm at the sides and 1.0 mm in the middle resulting in 67 257 elements with 92 019 nodes.

2.2.2 Boundary conditions

The rocker, support plate and clamping plates are treated as a single solid. Both blades are connected to the upper clamping plate by rigid multi-point constraints that enable transmission between the three degrees of freedom of the rigid body nodes and the six degrees of freedom of the shell element's flexible body nodes. Contact between the blades is implemented by means of a frictionless contact using the pure penalty method and the thickness effect of the shell elements to minimize unrealistic penetration and allow separation of the blades. A frictional contact with a coefficient of friction of $\mu = 0.01$ was specified for the contact between the doctor blade and the gravure cylinder. This is a first assumption for the lubricated contact in order to investigate changes in the loads in a transverse direction during the doctoring process until measurements are performed. Again, the pure penalty method and thickness effect of the shell elements are used.

Displacement of the components is constrained with respect to the coordinate systems as specified in Figure 2. All six degrees of freedom are restricted for the gravure cylinder at the bearing section. The movement of the doctoring unit is established by limiting all degrees of freedom except rotation around the y_0-axis and lateral movement in a y_0-direction. That movement is given by a sinusoidal displacement which simulates the eccentric drive of the gravure printing proofer. Displacement in an $x_0$direction is applied to the rocker lever, which increases the reaction force linearly until it reaches a maximum of 250 N. This pivots the doctoring unit. Gravitational loads are neglected at this stage. The load and displacement are applied subsequently in two timesteps. In the first timestep with a duration of one second the displacement is applied to the doctoring unit and both blades bend and press against the gravure cylinder. In the second timestep of one to two seconds a 5 mm lateral movement is performed to each side sinusoidally. The maximum offset positions are reached at 1.25 and 1.75 seconds.

3. Results and discussion

3.1 Results

In Figure 3 the results of the finite element analysis are presented for t = 1 s and t = 1.75 s. The undeformed wireframe of the geometry, as well as the gravure cylinder (top) and blade holder (bottom) are included in the figure for reference purposes. The results are described in further detail below.

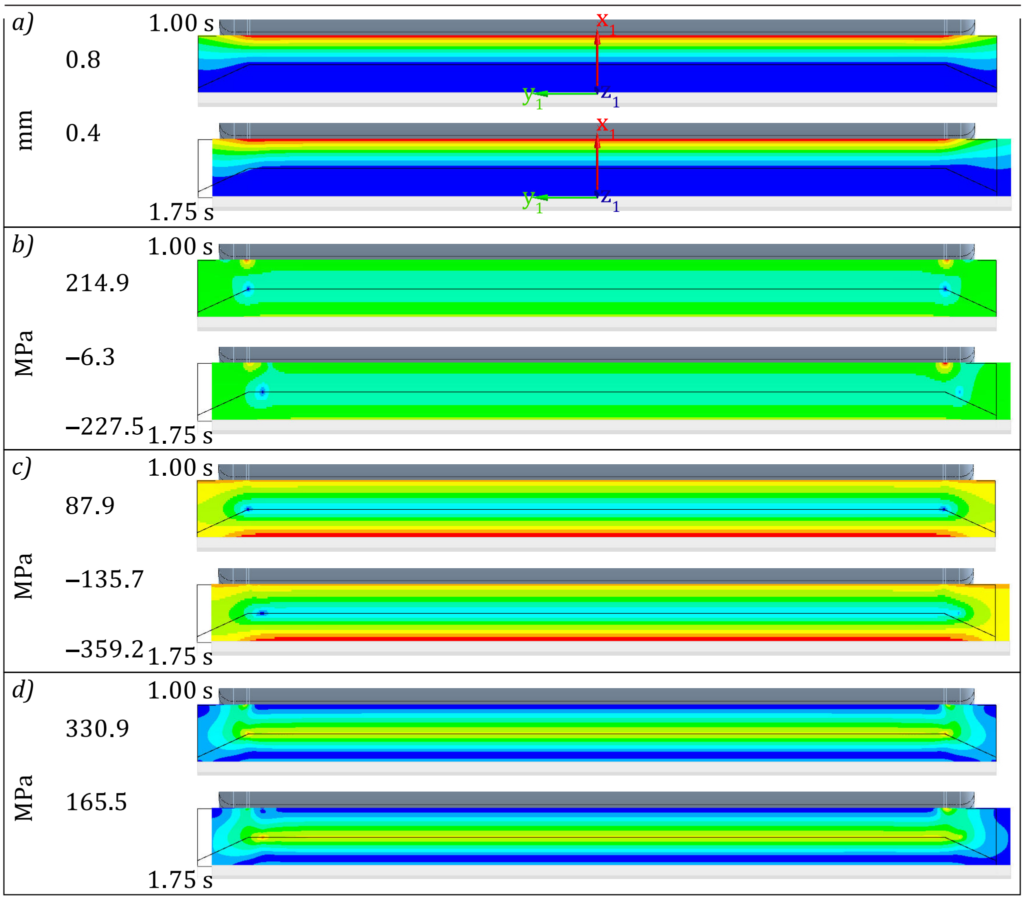

Figure 3: Results after t = 1 s and t = 1.75 s: (a) displacement in z_1-direction, (b) bending stress around the x_1-axis, (c) bending stress around the y_1-axis, (d) von Mises stress

Figure 3a shows the displacement in a $z_1$direction with respect to the local coordinate system defined at the clamped base of the blades, as shown in Figure 2. The deflection is constant over the cylindrical portion of the gravure cylinder. In contrast, less deflection can be observed at the extends of the doctor blade. The maximum deflection of u = 0.809 mm is located at the cylinder's left end at t = 1.75 s when moved inwards, while the deflection at the right end of the doctor blade decreases. This asymmetric displacement leads to asymmetric stresses while the doctoring unit is off-centred. Figures 3b and 3c present the bending stresses around the x_1-axis and y_1-axis at the top of the doctor blade. In the course of bending around the x_1-axis, high tensile stresses can be observed locally at the ends of the cylinder, where the doctor blade sides are bent downwards. The maximum tensile stress is $\sigma_{\mathrm{bt},x_1} = 214.9$ MPa at $t = 1.75$ s. Additionally, high compressive stresses with a maximum of $\sigma_{\mathrm{bc},x_1} = -227.5$ MPa can be observed for the same timestamp at the edge of the support blade, where it bends upwards. Around the y_1-axis tensile stresses appear at the clamped base of the blade where it deflects downwards, and compressive stresses appear at the contact with the support blade where it is bent upwards. At timestamp $t = 1.75$ s the maximum tensile stress is $\sigma_{\mathrm{bt},y_1} = 87.9$ MPa and the maximum compressive stress is $\sigma_{\mathrm{bc},y_1} = -359.2$ MPa. Figure 3d displays the von Mises stresses for the whole doctor blade. The position of the maximum von Mises stress with $\sigma_{\mathrm{vM}} = 330.9$ MPa is at the left edge of the support blade at $t = 1.75$ s.

3.2 Discussion

With the given simulation model and the results as shown in section 3.1, it can be stated that a quantitative evaluation of doctor blade deflection is achievable accurately. In contrast, evaluation of the stresses should be carried out qualitatively, especially in the contact region. This is because shear stresses are not included in the formulation of the shell elements. Furthermore, high stresses can be anticipated at the doctor blade tip due to the expected Hertzian pressure. The selected shell elements cannot resolve the contact area finely enough to represent the three-dimensional effects, as the height of the doctor blade is only represented by one element. This results in a singularity and a sensitivity of the stresses to the element size in the region of contact.

4. Conclusions and outlook

4.1 Conclusions

By including the lateral movement of the doctor blade unit in the numerical model of the doctoring process in gravure printing, it is shown that, as expected, high stresses appear at the gravure cylinder ends. However, in the given state of the model a quantitative evaluation is not reliable. It is reasonable that the highest stresses appear at the maximum offset positions of lateral movement because of the bevelled support blade and the maximum stiffness in that position. It can be concluded that modelling the doctor blade with shell elements can contribute to an understanding of the lateral movement, but further adaptation of the model is needed to account for all relevant physical effects.

4.2 Outlook

By extending the simulation model, the doctoring process can be analysed even more extensively. In order to simulate the process influence of the doctor blade geometry more precisely, the ground edge should be simulated via variable element thickness or volumetric 3D mesh. This will enable quantitative evaluation of the stresses and contact pressure of the doctor blade against the cylinder in greater detail. Besides this, sub-modelling techniques can be implemented to further improve the simulation model. For this purpose, it may also be useful to include geometric deviations of the cylinder. A promising approach here is the simulation of different process settings, which will facilitate sensitivity analysis with regard to the selected process parameters. These settings can also be reproduced on the laboratory printing machine, and the simulation model can thus be validated by strain gauge or optical measurements during the process. Further investigative approaches can be opened up by combined simulations including wear and flow behaviour.

Acknowledgements

The authors acknowledge TKM Meyer GmbH for bringing the problem to their attention, as well as providing the gravure printing proofer and partially funding the doctoral position of C.S. as part of a cooperative project.

Conflict of interest

The doctoral position of C.S. is partially funded by TKM Meyer GmbH whose parent company TKM GmbH is partly funding the doctoral position of T.S.. All other authors declare no conflict of interest. The funders had no influence on the design of the research, the simulation and interpretation of data, or the writing of the manuscript.

Contributions

Conceptual design, C.S., A.S. and T.S.; Investigation, C.S.; Modelling, C.S. and T.S.; Simulation, C.S.; Discussion of simulation results, C.S., A.S. and T.S.; Writing—original draft preparation, C.S., A.S. and T.S.; Writing—review and editing, C.S., A.S., T.S. and P.G.; Funding acquisition, P.G. and C.S.; Supervision, A.S. and P.G. All authors have read and agreed to the published version of the manuscript.

References

Bitsch, T., 2020. *Experimente zum Strömungs- und Benetzungsverhalten von Fluiden im Hochscherratenbereich am Beispiel des Rakelprozesses*. Ph.D. thesis. Technical University of Darmstadt. https://doi.org/10.26083/tuprints-00017589.

Bohan, M.F.J., Claypole, T.C. and Gethin, D.T., 2000. The effect of process parameters on product quality of rotogravure printing. *Proceedings of the Institution of Mechanical Engineers, Part B: Journal of Engineering Manufacture*. 214(3), pp. 205–219. https://doi.org/10.1243/0954405001517595.

Hanumanthu, R., 1999. Variation of gravure coating thickness during early stages of doctor blade wear. *AIChE Journal*, 45(12), pp. 2487–2494. https://doi.org/0.1002/aic.690451204.

Hoang, H.P. and Ko, S.L., 2015. Effect of doctoring on the performance of direct gravure printing for conductive microfine lines. *Journal of Micromechanics and Microengineering*, 25(11): 115018. https://doi.org/10.1088/0960-1317/25/11/115018.

Kipphan, H., 2001. Fundamentals. In: H. Kipphan, ed. *Handbook of print media: technologies and production methods*. Berlin, Heidelberg: Springer, pp. 1–201. https://doi.org/10.1007/978-3-540-29900-4_1.

Ollech, B., 1993. *Tiefdruck: Grundlagen und Verfahrensschritte der modernen Tiefdrucktechnik*. 2nd ed. Frankfurt am Main: Polygraph.

Scheuter, K.R. and Bognar, D., 1968. Beitrag zum Rakelproblem. *DRUCK-PRINT*, 105(4), pp. 293–299. https://doi.org/10.25534/TUPRINTS-00014126.

Swedev AB, Munkfors/S., 2011. Hart und dennoch flexibel - Wissenswertes über die Auswahl von Rakeln für den Tiefdruck. *Flexo+Tief-Druck*, 22(6), pp. 16–19.